

# Multi-photon Atom Interferometry via cavity-enhanced Bragg Diffraction

D. O. Sabulsky,<sup>1,\*</sup> J. Junca,<sup>1</sup> X. Zou,<sup>1</sup> A. Bertoldi,<sup>1</sup> M. Prevedelli,<sup>2</sup>  
Q. Beaufils,<sup>3</sup> R. Geiger,<sup>3</sup> A. Landragin,<sup>3</sup> P. Bouyer,<sup>1</sup> and B. Canuel<sup>1,†</sup>

(MIGA Consortium)

<sup>1</sup>*LP2N, Laboratoire Photonique, Numérique et Nanosciences,*

*Université Bordeaux-IOGS-CNRS:UMR 5298, rue F. Mitterrand, F-33400 Talence, France*

<sup>2</sup>*Dipartimento di Fisica e Astronomia, Università di Bologna, Via Bertini-Pichat 6/2, I-40126 Bologna, Italy*

<sup>3</sup>*LNE-SYRTE, Observatoire de Paris, Université PSL, CNRS,*

*Sorbonne Université, 61, avenue de l'Observatoire, F-75014 Paris, France*

(Dated: January 28, 2022)

Optical cavities are proposed as powerful tools for the realization of large momentum beam splitters for matter waves. In this letter, we realize a multi-photon atom interferometer driven via Bragg diffraction in an optical resonator. The key element of this demonstration is the use of a degenerate cavity to mediate the light-matter interaction, which provides a large interrogation mode ( $1/e^2$  diameter of 5.3 mm) and makes the method applicable to a vast class of measurement geometries and atomic sources. In view of a future application for gravitational wave observation, we use, as a first demonstration, an 80 cm horizontal resonator coupled with a standard sub-Doppler cooled Rb atomic source and observe momentum transfer up to  $8\hbar k$ . We demonstrate the inertial sensitivity of this setup using significantly reduced optical power ( $\approx 1$  mW) due to the optical gain of the cavity. This work opens new perspectives not only for the realization of high sensitivity multi-axis inertial atom sensors, but also for the future realization of hybrid atom/optical gravitational wave detectors.

Long baseline atom interferometry has seen growing interest due to its potential for breakthroughs in multiple fields, of note being terrestrial and space-based decihertz gravitational wave observation [1–6], dark matter observation [7, 8], precision mapping of static, as well as dynamic, mass distributions [1, 9], and tests of the equivalence principle [10, 11]. This new generation of high precision detectors share a common philosophy: a network of atom interferometers are simultaneously interrogated by the same optical pulse. Various techniques are proposed, in combination, to reach the projected sensitivity required for these high precision tests - bright atomic flux [12, 13], interleaved interferometers [14], entangled sources [15, 16], but also large momentum transfer (LMT) atom optics. In such experiments, the sensitivity of the measurement fundamentally depends on the spatial separation of matter waves inside the interferometer, which is commonly limited by the use of 2-photon momentum transfer from the interrogation field to the atoms. Various LMT schemes have been studied, enabling atom interferometer experiments to multiply the number of photons exchanged, and thus increase their sensitivity linearly, by factors up to a thousand [17–25].

Increasing recoil momentum  $n\hbar k$  to large  $n$  [19] via coherent multi-photon interactions poses strong constraints on laser power and stability [26]. To overcome the direct generation of low-noise yet high-power lasers, stable optical resonators have been proposed to provide so-called cavity enhancement.

An optical resonator cleans the spatial mode of the beam, increases the circulating optical intensity, and maintains the required polarization and wave vectors.

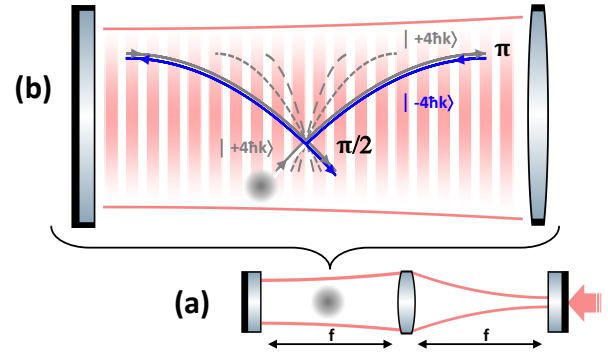


FIG. 1. (a) Degenerate resonator geometry using a two plane mirrors at a focal plane of an intra-cavity lens that interrogates an atom source (grey). (b) Geometry of the  $\pi/2 - \pi - \pi/2$  Mach-Zehnder atom interferometer using Bragg diffraction on the cavity standing wave (red) and manipulating the momentum states  $|\pm n\hbar k\rangle$ . The splitting of matter-waves scales with the momentum transfer (grey dashed lines  $2n = 2$  and  $4\hbar k$ , grey and blue plain lines  $8\hbar k$ ).

Despite these potential improvements, the efficiency of cavity interrogation scales with the resonator length and finesse, with high efficiency tending towards short linewidth cavities with a long temporal response. Such a response degrades the shape of the light pulses used to coherently manipulate the matter waves [28]. While these effects were considered, up to now, as a fundamental issue limiting the use of optical cavities for atom interferometry [26], novel schemes were recently proposed to circumvent this problem using light-shift engineering [29] and intracavity frequency modulation on circulating pulses [30]. To date, an experimental demonstration

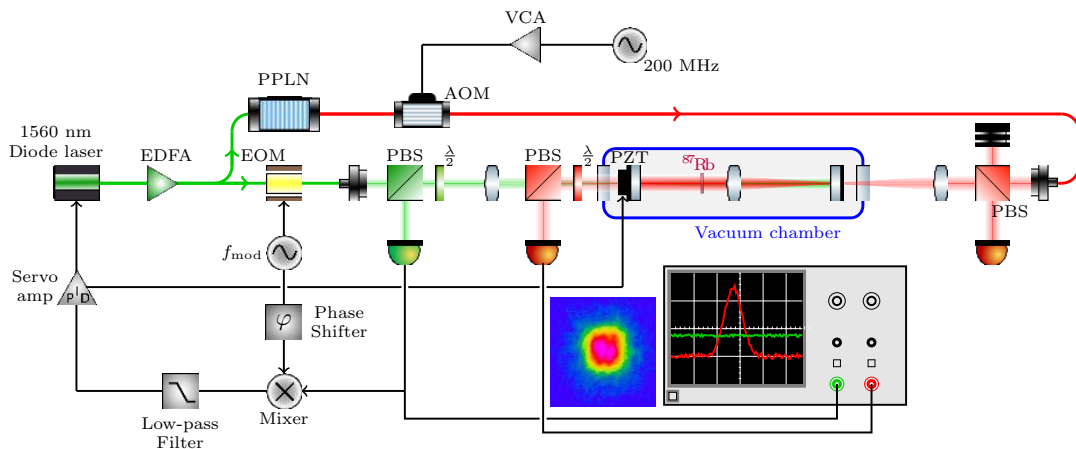


FIG. 2. Degenerate optical resonator schematic. We inject Gaussian beams at 1560 nm and 780 nm into the horizontal optical resonator; they are intrinsically phase locked as they are derived from the same source. The 1560 nm beam follows the same path but reversed, and is used to length-frequency stabilize the cavity with the piezo. The beam profile in transmission is shown next to a resonance at 780 nm indicative of good alignment [27].

[31] of a  $2\hbar k$  cavity atom interferometer was realized in a configuration where atoms are trapped efficiently in the small mode volume ( $600 \mu\text{m}$ ) of a stable resonator. In a more recent work, a stable high finesse optical cavity was used for entanglement enhancement of atom interferometry [16].

In this letter, we realize the demonstration of large momentum transfer in a configuration where the atom-light interaction is mediated using a degenerate resonator. This configuration, previously studied in [27, 32], comprises two high reflectivity mirrors placed at the focal planes of a lens. This degenerate geometry [33] allows for the propagation of large, arbitrary spatial modes, making the method applicable to a vast class of measurement geometries and atomic sources such as free falling laser cooled atom sources commonly used in metrological atomic experiments. We use an 80 cm horizontal resonator coupled with a sub-Doppler cooled  $^{87}\text{Rb}$  atomic source, shown in Fig. 1, and create a Mach-Zehnder  $\pi/2 - \pi - \pi/2$  matter wave interferometer using a momentum transfer of up to  $2n = 8\hbar k$  on a large resonating mode with a  $1/e^2$  diameter of 5.3 mm. We first show the inertial sensitivity of the device via a tilt experiment [22, 34]. We then move to demonstrate multi-photon diffraction, first focusing on monochromatic Bragg diffraction up to order four ( $n = 4$ ) and discussing the limitation of population transfer efficiency. We finish by demonstrating interference with up to  $8\hbar k$  splitting and studying the scale factor variation of the interferometer.

We have described the optical cavity [27, 32], and cold atom system [1, 9, 35] used in this experiment elsewhere. We now describe the functioning of the Bragg diffraction laser, shown in Fig. 2. This system is based on a fibered laser diode centered at 1560 nm with a characteristic linewidth (Lorentzian FWHM) of 4.30 kHz.

This laser seeds a high-power dual-stage Erbium-doped fiber amplifier which in turn pumps a periodically-poled Lithium-Niobate crystal, all shunted over polarization-maintaining fibers, generating the 780 nm interrogation light. The 1560 nm and 780 nm lasers are injected into opposite cavity ports. Fine alignment of the optical cavity is achieved using UHV-compatible linear piezo actuators, with step resolution  $< 30 \text{ nm}$ , contained within kinematic mirror mounts. To exercise complete control, we employ three actuators on the injection mirror for 780 nm and two actuators and a bored cylindrical piezoelectric transducer stack on the reflecting mirror.

We servo the 1560 nm diode laser to the resonator via phase modulation of a fibered EOM, utilizing the Pound-Drever-Hall technique [36] - we send fast feedback on the laser diode current and, to limit large DC actuation of this current, send slow feedback to the cavity piezostack (PZT). The frequency doubled light at 780 nm is modulated by a fibered AOM to generate the interrogation pulses. We use a Gaussian amplitude modulation of a sinusoidal carrier produced by an arbitrary function generator. We emphasize that, in this laser architecture, the interrogation and cavity control lasers are naturally phase coherent which make it significantly simpler than the systems reported previously for stable cavities [31]. Further, the marginally stable architecture is one that can freely adapt to various resonating mode sizes whose control frequency is arbitrary. This can improve the systematic errors introduced by the control laser during interrogation.

The cavity optics comprise two 25 mm flat mirrors of RMS flatness 44 pm and 52 pm and one 50 mm convex-convex lens of focal length 400 mm, with peak to peak surface irregularities of 118 nm (face 1) and 206 nm (face 2); we have deviated from our previous work [32], choos-

ing a biconvex lens over a plano-convex to ensure injection symmetry for stabilizing the laser to the cavity. The mirrors are coated with a 0 degree angle-of-incidence high-reflectivity dielectric coating (99.69% at both 780 nm and 1560 nm) on one side and 0 degree angle-of-incidence anti-reflection coating (0.015% at 780 nm and 0.014% at 1560 nm) on the other. We utilize a pseudo-TEM<sub>00</sub> spatial mode by injecting a Gaussian beam focused down to a spot characterized by a  $1/e^2$  diameter of 75  $\mu\text{m}$ . Based on the parameters of the three optics that comprise the optical cavity, we predict a maximum gain and finesse of  $G_{\text{max}} \simeq 49$  and  $\mathcal{F}_{\text{max}} \simeq 260$  with a resonating beam diameter above 10 mm; our previous work showed that the resonator parameters are highly dependent upon misalignment and optical imperfections [27, 32], which is corroborated by our measurements,  $G = 38$  and  $\mathcal{F} = 200$  with a maximum resonating beam diameter of 5.3 mm. The optical gain of the resonator is sufficient to drive diffraction with mW level input from a low-noise source, while the finesse results in a cavity temporal response of 0.17  $\mu\text{s}$ , sufficiently low to not distort the applied Gaussian pulses.

We launch a thermal cloud of atoms into the cavity by first preparing a few  $10^6$   $^{87}\text{Rb}$  atoms at 2.9  $\mu\text{K}$  with a vertical velocity of  $v = 3.709$  m/s in the magnetically-insensitive Zeeman sublevel ( $m_F = 0$ ) of the  $F = 1$  hyperfine ground state - these atoms have been subjected to a severe velocity pre-selection on their ballistic trajectory, where their momentum distribution along the interrogation axis can be described by  $T = 58$  nK. The atomic ensemble's center-of-mass ballistic trajectory intersects the optical axis of the resonator at the apogee, where we interrogate the atomic sample. The Bragg laser system is blue-detuned by  $\Delta = 3.6$  GHz relative to the  $F = 1 \rightarrow F' = 2$  transition in  $^{87}\text{Rb}$ . We apply the interrogation pulses with a Gaussian time envelope,  $f(t) = \text{Exp}[-t^2/2\sigma^2]$ , that is proven to enhance the efficiency of LMT beam splitters [37]; this is a so-called “quasi-Bragg” scattering regime characterized by short interaction times and negligible losses to intermediate momentum states. After interrogation, the atoms follow a modified ballistic trajectory, where the external momentum state populations are given separate internal energy states via Raman transition and then measured via fluorescence detection, see (a) of Fig. 3; a similar detection scheme can be found in [38]. By scanning the 2-photon detuning of the Raman beam, we perform momentum spectroscopy to observe our thermal cloud and diffracted atoms. In short, after interrogation and state labeling, the atoms fall through three light sheets, slightly blue-detuned to the  $F = 2 \rightarrow F' = 3$  (top and bottom) and  $F = 1 \rightarrow F' = 2$  (middle) transition of  $^{87}\text{Rb}$  and at a saturation parameter  $s$  of around 1. As the atoms pass, we observe a lineshape on two perpendicular quadrant photodiodes; it is the convolution of the width of the beam and the spatial extent of the cloud.

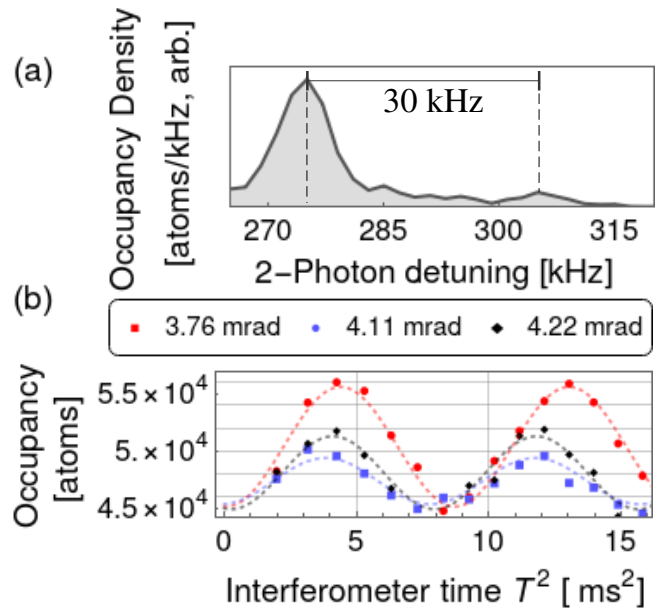


FIG. 3. Bragg diffraction and interference inside the resonator. (a) Raman spectroscopy after single Bragg diffraction for a  $\pi$  pulse, for a tilt of 4.22 mrad. (b) To observe interference, we change the scale factor by varying the interferometer time  $T$ . For varying tilt angle, we observe a cantilevering effect from a finite projection with gravity that changes the inter-fringe spacing.

The shape is affected by the velocity of the cloud passing through the sheets, and so is a function of launch height / velocity, and temperature.

We start by demonstrating atomic interference and inertial sensitivity using a standard  $2\hbar k$  interferometer. We first establish a  $\pi$  pulse for single diffraction by optimizing transfer into our target momentum state, see (a) of Fig. 3, where we transfer  $9 \times 10^4$  atoms from the  $|\hbar\mathbf{k}\rangle$  to the  $|\hbar\mathbf{k}\rangle$  state, an efficiency of  $\simeq 20\%$ , for a pulse of 102  $\mu\text{s}$ . We expect to observe this momentum state occupation at a frequency  $\nu_0 + 2n\nu_{\text{rec}}$  where  $\nu_0$  is related to the momentum of the cloud  $\nu_{\text{rec}} = 15.084$  kHz is the recoil frequency for the  $^{87}\text{Rb}$  D2 transition. Following these optimizations, we check for intermediate state occupancy, finding only a few percent above the background. We then apply a sequence of cavity pulses  $\pi/2 - \pi - \pi/2$  separated by time  $T$  to generate an interferometer. By tilting the experiment by an angle  $\alpha$ , we vary the projection of local gravity  $g$  along the interrogation field and create an atomic phase difference of  $2n\alpha g k T^2$ . We can then observe interference patterns by changing the scale factor  $T^2$  of the interferometer, see (b) of Fig. 3. This experiment is repeated for different tilts of the setup - the inter-fringe measurement enables us to recover the tilt angles using the value of local gravity determined five meters away, horizontally translated, from our experiment [39]. We compare the tilt measured by the atoms to that

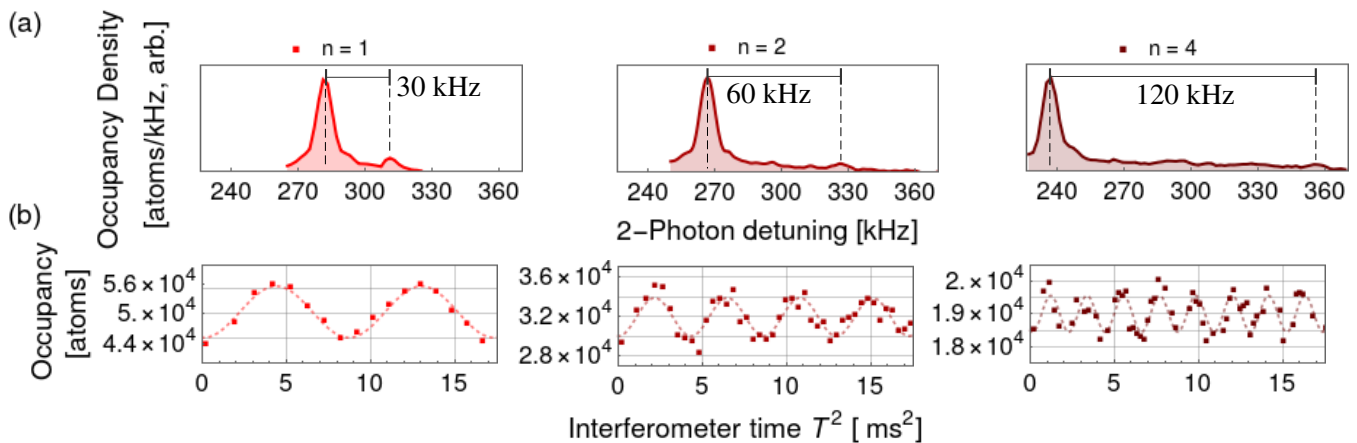


FIG. 4. Multi-photon monochromatic diffraction and fringes inside a degenerate resonator via scale factor variation. (a) We perform Raman spectroscopy after Bragg diffraction to observe external momentum state occupation. From left to right, in increasingly dark shades of red, we show  $n = 1, 2, 4$ ; each point is an average of 3 measurements. (b) We vary the time  $T$  of the interferometer and show interference for  $n = 1, 2, 4$ , from left to right, in increasingly dark shades of red and for a fixed tilt angle of 3.76 mrad. The light dashed lines are fits of the fringe patterns, weighted with the error of each point; each point is an average of 20 measurements.

of an interferometric laser level and found agreement to within error. The total angle variation we applied ( $0.46 \text{ mrad} \pm 0.19 \text{ mrad}$ ) is limited by the strong effects this has on the interferometric contrast through modification of the ballistic trajectory of the atoms.

In the tilt test, we found that the diffraction efficiency is limited by a maximum resonating waist smaller than the one predicted. By empirical variation of the input diameter, we arrived at  $\omega = 5.3 \text{ mm}$  as it is the largest input waist diameter that can resonate before the internal beam is clipped; further, to increase the beam waist past this point decreased the gain of resonator. Our previous work [32] led us to understand this significant limitation, in that the small resonating waist is a consequence of both longitudinal spherical aberration and astigmatism induced by the lens; the gain and finesse measurements

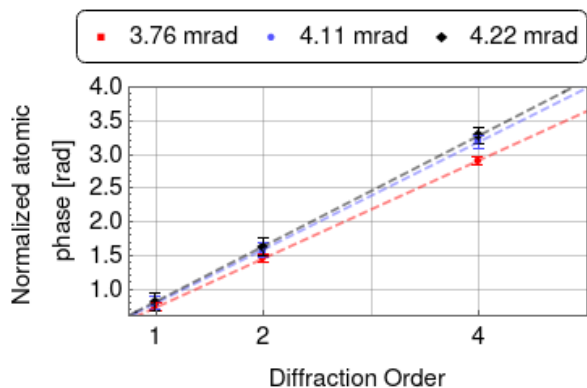


FIG. 5. Inertial sensitivity via tilt measurement. We compare the normalized atomic phase for increasing diffraction order and tilt angle.

and their difference from predicted values corroborate this inference.

We now present multi-photon diffraction with this setup. We first inspect our Bragg diffraction inside the resonator for monochromatic driving, see (a) of Fig. 4. We perform Raman spectroscopy after Bragg diffraction to determine momentum state occupancy, observing minor spurious excitation past the targeted momentum state. The observed limitation of transfer efficiency is primarily due to the size of the resonating waist, from 18% for  $n = 1$ , to 16% for  $n = 2$ , down to 12% for  $n = 4$ . The optical power injected into the resonator required for a  $\pi$ -pulse ranges from 1 mW for  $n = 1$ , 3 mW for  $n = 2$ , to 18 mW for  $n = 4$  - a Gaussian beam of similar size would need well over 700 mW to drive diffraction. We use a  $\pi$ -pulse duration for  $n = 1, 2, 4$  corresponding to 102  $\mu\text{s}$ , 51  $\mu\text{s}$ , and 32  $\mu\text{s}$  respectively. We then apply a sequence of cavity pulses  $\pi/2 - \pi - \pi/2$  and observe interference patterns by changing the interaction time  $T^2$  for a given tilt of the setup. This experiment is repeated for the different target momentum states  $n = 1, 2, 4$  from left to right in (b) of Fig. 4. The reduction in participating atoms for increasing  $n$  is expected [27, 32]; in the quasi Bragg regime, the transfer of atoms to the target momentum state is a non-linear process - for an increasing effective Rabi frequency  $\Omega_{\text{eff}}$  [19, 27], the process becomes highly sensitive to transverse intensity inhomogeneity. This is to say that to target increasing diffraction order  $n$  with a coherent transfer process, the efficiency of Bragg diffraction becomes increasingly dependent upon and sensitive to intensity variations.

In (b) of Fig. 4, we observe a reduction of the spacing between fringes as a function of the targeted momentum state, which shows the improvement of the measurement

scale. We studied this variation for three different tilts of the experiment, see Fig. 5. The three sets of measurements agrees with a linear increase of the measurement scale factor as a function of  $n$ , which is expected for LMT interferometry.

In this letter, we have demonstrated multi-photon atom interferometry inside an optical resonator and show that this system is inertially sensitive via tilt experiment. This work paves the way towards increased sensitivity of matter wave interferometer experiments. In particular, atom interferometry is now being considered to build large scale detectors for the observation of gravitational waves and the study of dark matter [4, 5, 40, 41]. Such experiments would use interrogation beams tens of kilometer long in the horizontal direction and resonators could be a key technique for their realization. A key aspect of our demonstration is the use of a degenerate cavity to mediate the light-matter interaction. This provides a flexible resonating mode which makes the entire cavity volume potentially usable for atom interrogation, unlike a stable cavity, where efficient interaction is restricted to small mode volumes. This method is therefore applicable to various atom interferometer sources and geometries, like mobile, sub-Doppler cooled vertical gravimeters [39] and horizontal gyroscopes [42].

The authors would like thank I. Riou, G. Lefèvre, and N. Mielec for their early work on the experiment. We gratefully acknowledge the engineering support of P. Teulat and L. Sidorenkov. J.J. thanks the “Association Nationale de la Recherche et de la Technologie” for financial support (N° 2018/1565). X.Z. thanks the China Scholarships Council (N° 201806010364) program for financial support. This work was realized with the financial support of the French State through the “Agence Nationale de la Recherche” (ANR) within the framework of the “Investissement d’Avenir” programs Equipex MIGA (ANR-11-EQPX-0028) and IdEx Bordeaux - LAPHIA (ANR-10-IDEX-03-02). This work was also supported by the région d’Aquitaine (project IASIG-3D and USOFF). We also acknowledge support from the CPER LSBB2020 project; funded by the “région PACA”, the “département du Vaucluse”, and the “FEDER PA0000321 programmation 2014-2020”. And finally, we acknowledge financial support from Ville de Paris (project HSENS-MWGRAV) and Agence Nationale pour la Recherche (project PIMAI, ANR-18-CE47-0002-01).

---

\* [dylan.banahene-sabulsky@institutoptique.fr](mailto:dylan.banahene-sabulsky@institutoptique.fr)

† [benjamin.canuel@institutoptique.fr](mailto:benjamin.canuel@institutoptique.fr)

- [1] B. Canuel, A. Bertoldi, L. Amand, E. P. di Borgo, T. Chantrait, C. Danquigny, M. D. Álvarez, B. Fang, A. Freise, R. Geiger, J. Gillot, S. Henry, J. Hinderer, D. Holleville, J. Junca, G. Lefèvre, M. Merzougui, N. Mielec, T. Monfret, S. Pelisson, M. Prevedelli, S. Reynaud,

- I. Riou, Y. Rogister, S. Rosat, E. Cormier, A. Landragin, W. Chaibi, S. Gaffet, and P. Bouyer, Exploring gravity with the MIGA large scale atom interferometer, *Sci. Rep.* **8**, 14064 (2018).
- [2] B. Canuel, The matter-wave laser interferometer gravitation antenna (MIGA): New perspectives for fundamental physics and geosciences, *E3S Web of Conf.* **4**, 01004 (2014).
- [3] J. Coleman, MAGIS-100 at Fermilab, in *Proceedings of The 39th International Conference on High Energy Physics — PoS(ICHEP2018)* (Sissa Medialab, 2019).
- [4] B. Canuel, S. Abend, P. Amaro-Seoane, F. Badaracco, Q. Beaufiles, A. Bertoldi, K. Bongs, P. Bouyer, C. Braxmaier, W. Chaibi, N. Christensen, F. Fitzek, G. Flouris, N. Gaaloul, S. Gaffet, C. L. G. Alzar, R. Geiger, S. Guellati-Khelifa, K. Hammerer, J. Harms, J. Hinderer, M. Holynski, J. Junca, S. Katsanevas, C. Klempt, C. Kozanitis, M. Krutzik, A. Landragin, I. L. Roche, B. Leykauf, Y.-H. Lien, S. Loriani, S. Merlet, M. Merzougui, M. Nofrarias, P. Papadakos, F. P. dos Santos, A. Peters, D. Plexousakis, M. Prevedelli, E. M. Rasel, Y. Rogister, S. Rosat, A. Roura, D. O. Sabulsky, V. Schkolnik, D. Schlippert, C. Schubert, L. Sidorenkov, J.-N. Siemß, C. F. Sopena, F. Sorrentino, C. Struckmann, G. M. Tino, G. Tsagkatakis, A. Viceré, W. von Klitzing, L. Woerner, and X. Zou, ELGAR—a European Laboratory for Gravitation and Atom-interferometric Research, *Classical and Quantum Gravity* **37**, 225017 (2020).
- [5] L. Badurina, E. Bentine, D. Blas, K. Bongs, D. Bortolotto, T. Bowcock, K. Bridges, W. Bowden, O. Buchmueller, C. Burrage, J. Coleman, G. Elertas, J. Ellis, C. Foot, V. Gibson, M. Haehnel, T. Harte, S. Hedges, R. Hobson, M. Holynski, T. Jones, M. Langlois, S. Lelouch, M. Lewicki, R. Maiolino, P. Majewski, S. Malik, J. March-Russell, C. McCabe, D. Newbold, B. Sauer, U. Schneider, I. Shipsey, Y. Singh, M. Uchida, T. Valenzuela, M. van der Grinten, V. Vaskonen, J. Vossebeeld, D. Weatherill, and I. Wilmut, AION: an atom interferometer observatory and network, *Journal of Cosmology and Astroparticle Physics* **5** (11), 2020.
- [6] D. Schlippert, C. Meiners, R. Rengelink, C. Schubert, D. Tell, É. Wodey, K. Zipfel, W. Ertmer, and E. Rasel, Matter-wave interferometry for inertial sensing and tests of fundamental physics, in *CPT and Lorentz Symmetry* (WORLD SCIENTIFIC, 2020).
- [7] Y. A. El-Neaj, C. Alpigiani, S. Amairi-Pyka, H. Araújo, A. Balaž, A. Bassi, L. Bathe-Peters, B. Battelier, A. Belić, E. Bentine, J. Bernabeu, A. Bertoldi, R. Bingham, D. Blas, V. Bolpasi, K. Bongs, S. Bose, P. Bouyer, T. Bowcock, W. Bowden, O. Buchmueller, C. Burrage, X. Calmet, B. Canuel, L.-I. Caramete, A. Carroll, G. Cella, V. Charmandaris, S. Chattopadhyay, X. Chen, M. L. Chiofalo, J. Coleman, J. Cotter, Y. Cui, A. Derevianko, A. De Roeck, G. S. Djordjevic, P. Dornan, M. Doser, I. Drougkakis, J. Dunningham, I. Duttan, S. Easo, G. Elertas, J. Ellis, M. El Sawy, F. Fassi, D. Felea, C.-H. Feng, R. Flack, C. Foot, I. Fuentes, N. Gaaloul, A. Gauguier, R. Geiger, V. Gibson, G. Giudice, J. Goldwin, O. Grachov, P. W. Graham, D. Grasso, M. van der Grinten, M. Gündogan, M. G. Haehnel, T. Harte, A. Hees, R. Hobson, J. Hogan, B. Holst, M. Holynski, M. Kasevich, B. J. Kavanagh, W. von Kl-

- itzing, T. Kovachy, B. Krikler, M. Krutzik, M. Lewicki, Y.-H. Lien, M. Liu, G. G. Luciano, A. Magnon, M. A. Mahmoud, S. Malik, C. McCabe, J. Mitchell, J. Pahl, D. Pal, S. Pandey, D. Papazoglou, M. Paternostro, B. Penning, A. Peters, M. Prevedelli, V. Puthiya-Veettill, J. Quenby, E. Rasel, S. Ravenhall, J. Ringwood, A. Roura, D. Sabulsky, M. Sameed, B. Sauer, S. A. Schäffer, S. Schiller, V. Schkolnik, D. Schlippert, C. Schubert, H. R. Sfar, A. Shayeghi, I. Shipsey, C. Signorini, Y. Singh, M. Soares-Santos, F. Sorrentino, T. Sumner, K. Tassis, S. Tentindo, G. M. Tino, J. N. Tinsley, J. Unwin, T. Valenzuela, G. Vasilakis, V. Vaskonen, C. Vogt, A. Webber-Date, A. Wenzlawski, P. Windpassinger, M. Wolzmann, E. Yazgan, M.-S. Zhan, X. Zou, and J. Zupan, AEDGE: Atomic Experiment for Dark Matter and Gravity Exploration in Space, *EPJ Quantum Technology* **7**, 6 (2020).
- [8] L. Badurina, D. Blas, and C. McCabe, Refined ultraviolet scalar dark matter searches with compact atom gradiometers, *Phys. Rev. D* **105**, 023006 (2022).
- [9] B. Canuel, S. Pelisson, L. Amand, A. Bertoldi, E. Cormier, B. Fang, S. Gaffet, R. Geiger, J. Harms, D. Holleville, A. Landragin, G. Lefèvre, J. Lhermite, N. Mielec, M. Prevedelli, I. Riou, and P. Bouyer, MIGA: combining laser and matter wave interferometry for mass distribution monitoring and advanced geodesy, *Proc. SPIE* **9900**, 990008 (2016).
- [10] C. Overstreet, P. Asenbaum, T. Kovachy, R. Notermans, J. M. Hogan, and M. A. Kasevich, Effective inertial frame in an atom interferometric test of the equivalence principle, *Phys. Rev. Lett.* **120**, 183604 (2018).
- [11] P. Asenbaum, C. Overstreet, M. Kim, J. Curti, and M. A. Kasevich, Atom-interferometric test of the equivalence principle at the  $10^{-12}$  level, *Phys. Rev. Lett.* **125**, 191101 (2020).
- [12] S. Loriani, D. Schlippert, C. Schubert, S. Abend, H. Ahlers, W. Ertmer, J. Rudolph, J. M. Hogan, M. A. Kasevich, E. M. Rasel, and N. Gaaloul, Atomic source selection in space-borne gravitational wave detection, *New Journal of Physics* **21**, 063030 (2019).
- [13] B. Canuel, S. Abend, P. Amaro-Seoane, F. Badaracco, Q. Beaufils, A. Bertoldi, K. Bongs, P. Bouyer, C. Braxmaier, W. Chaibi, N. Christensen, F. Fitzek, G. Flouris, N. Gaaloul, S. Gaffet, C. L. G. Alzar, R. Geiger, S. Guellati-Khelifa, K. Hammerer, J. Harms, J. Hinderer, M. Holynski, J. Junca, S. Katsanevas, C. Klempt, C. Kozanitis, M. Krutzik, A. Landragin, I. L. Roche, B. Leykauf, Y. H. Lien, S. Loriani, S. Merlet, M. Merzougui, M. Nofrarias, P. Papadakos, F. P. dos Santos, A. Peters, D. Plexousakis, M. Prevedelli, E. M. Rasel, Y. Rogister, S. Rosat, A. Roura, D. O. Sabulsky, V. Schkolnik, D. Schlippert, C. Schubert, L. Sidorenkov, J. N. Siemß, C. F. Sopaerta, F. Sorrentino, C. Struckmann, G. M. Tino, G. Tsagkatakis, A. Viceré, W. von Klitzing, L. Woerner, and X. Zou, Technologies for the ELGAR large scale atom interferometer array (2020), [arXiv:2007.04014 \[physics.atom-ph\]](https://arxiv.org/abs/2007.04014).
- [14] D. Savoie, M. Altorio, B. Fang, L. A. Sidorenkov, R. Geiger, and A. Landragin, Interleaved atom interferometry for high-sensitivity inertial measurements, *Science Advances* **4**, eaau7948 (2018).
- [15] F. Anders, A. Idel, P. Feldmann, D. Bondarenko, S. Loriani, K. Lange, J. Peise, M. Gersemann, B. Meyer-Hoppe, S. Abend, N. Gaaloul, C. Schubert, D. Schlippert, L. Santos, E. Rasel, and C. Klempt, Momentum entanglement for atom interferometry, *Phys. Rev. Lett.* **127**, 140402 (2021).
- [16] G. P. Greve, C. Luo, B. Wu, and J. K. Thompson, Entanglement-enhanced matter-wave interferometry in a high-finesse cavity (2021), [arXiv:2110.14027 \[quant-ph\]](https://arxiv.org/abs/2110.14027).
- [17] J. McGuirk, M. Snadden, and M. Kasevich, Large area light-pulse atom interferometry, *Phys. Rev. Lett.* **85**, 4498 (2000).
- [18] M. Cadoret, E. de Mirandes, P. Cladé, S. Guellati-Khelifa, C. Schwob, F. Nez, L. Julien, and F. Biraben, Combination of Bloch oscillations with a Ramsey-Bordé interferometer: New determination of the fine structure constant, *Phys. Rev. Lett.* **101**, 230801 (2008).
- [19] H. Müller, S.-W. Chiow, Q. Long, S. Herrmann, and S. Chu, Atom interferometry with up to 24-photon-momentum-transfer beam splitters, *Phys. Rev. Lett.* **100**, 180405 (2008).
- [20] H. Müller, S.-w. Chiow, S. Herrmann, and S. Chu, Atom interferometers with scalable enclosed area, *Phys. Rev. Lett.* **102**, 240403 (2009).
- [21] T. Kovachy, Quantum superposition at the half-metre scale, *Nature* **528**, 10.1038/nature16155 (2015).
- [22] H. Ahlers, H. Müntinga, A. Wenzlawski, M. Krutzik, G. Tackmann, S. Abend, N. Gaaloul, E. Giese, A. Roura, R. Kuhl, C. Lämmerzahl, A. Peters, P. Windpassinger, K. Sengstock, W. P. Schleich, W. Ertmer, and E. M. Rasel, Double Bragg interferometry, *Phys. Rev. Lett.* **116**, 173601 (2016).
- [23] M. Jaffe, V. Xu, P. Haslinger, H. Müller, and P. Hamilton, Efficient adiabatic spin-dependent kicks in an atom interferometer, *Phys. Rev. Lett.* **121**, 040402 (2018).
- [24] G. M. S. Abend, J.-N. Siemß, M. Gersemann, H. Ahlers, H. Müntinga, S. Herrmann, N. Gaaloul, C. Schubert, K. Hammerer, C. Lämmerzahl, W. Ertmer, and E. Rasel, Twin-lattice atom interferometry, *arXiv preprint arXiv:1907.08416* (2019).
- [25] Z. Pagel, W. Zhong, R. H. Parker, C. T. Olund, N. Y. Yao, and H. Müller, Symmetric Bloch oscillations of matter waves, *Phys. Rev. A* **102**, 053312 (2020).
- [26] M. Dovale-Álvarez, D. D. Brown, A. W. Jones, C. M. Mow-Lowry, H. Miao, and A. Freise, Fundamental limitations of cavity-assisted atom interferometry, *Phys. Rev. A* **96**, 053820 (2017).
- [27] I. Riou, N. Mielec, G. Lefèvre, M. Prevedelli, A. Landragin, P. Bouyer, A. Bertoldi, R. Geiger, and B. Canuel, A marginally stable optical resonator for enhanced atom interferometry, *Journal of Physics B: Atomic, Molecular and Optical Physics* **50**, 155002 (2017).
- [28] B. Fang, Improving the phase response of an atom interferometer by means of temporal pulse shaping, *New J. Phys.* **20**, 10.1088/1367-2630/aaa37c (2018).
- [29] A. Bertoldi, C.-H. Feng, D. Naik, B. Canuel, P. Bouyer, and M. Prevedelli, Fast control of atom-light interaction in a narrow linewidth cavity, *Physical Review Letters* **127**, 013202 (2021).
- [30] R. Nourshargh, S. Lellouch, S. Hedges, M. Langlois, K. Bongs, and M. Holynski, Circulating pulse cavity enhancement as a method for extreme momentum transfer atom interferometry, *Communications Physics* **4**, 257 (2021).
- [31] P. Hamilton, M. Jaffe, J. M. Brown, L. Maisenbacher, B. Estey, and H. Müller, Atom interferometry in an opti-

- cal cavity, *Physical Review Letters* **114**, 100405 (2015).
- [32] N. Mielec, R. Sapam, C. Poulain, A. Landragin, A. Bertoldi, P. Bouyer, B. Canuel, and R. Geiger, Degenerate optical resonator for the enhancement of large laser beams, *Opt. Express* **28**, 39112 (2020).
- [33] J. Arnaud, Degenerate optical cavities, *Applied optics* **8**, 189–195 (1969).
- [34] J. Liu, W.-J. Xu, C. Zhang, Q. Luo, Z.-K. Hu, and M.-K. Zhou, Sensitive quantum tiltmeter with nanoradian resolution, *Phys. Rev. A* **105**, 013316 (2022).
- [35] D. O. Sabulsky, J. Junca, G. Lefèvre, X. Zou, A. Bertoldi, B. Battelier, M. Prevedelli, G. Stern, J. Santoire, Q. Beauvils, R. Geiger, A. Landragin, B. Desruelle, P. Bouyer, and B. Canuel, A fibered laser system for the MIGA large scale atom interferometer, *Scientific Reports* **10**, 3268 (2020).
- [36] R. W. P. Drever, J. L. Hall, F. V. Kowalski, J. Hough, G. M. Ford, A. J. Munley, and H. Ward, Laser phase and frequency stabilization using an optical resonator, *Applied Physics B* **31**, 97 (1983).
- [37] H. Müller, S. Chiow, and S. Chu, Atom-wave diffraction between the Raman-Nath and the Bragg regime: Effective Rabi frequency, losses, and phase shifts, *Phys. Rev. A* **77**, 023609 (2008).
- [38] Y. Cheng, K. Zhang, L.-L. Chen, T. Zhang, W.-J. Xu, X.-C. Duan, M.-K. Zhou, and Z.-K. Hu, Momentum-resolved detection for high-precision bragg atom interferometry, *Phys. Rev. A* **98**, 043611 (2018).
- [39] V. Ménot, P. Vermeulen, N. L. Moigne, S. Bonvalot, P. Bouyer, A. Landragin, and B. Desruelle, Gravity measurements below  $10^{-9} g$  with a transportable absolute quantum gravimeter, *Sci. Rep.* **8**, 12300 (2018).
- [40] M.-S. Zhan, J. Wang, W.-T. Ni, D.-F. Gao, G. Wang, L.-X. He, R.-B. Li, L. Zhou, X. Chen, J.-Q. Zhong, B. Tang, Z.-W. Yao, L. Zhu, Z.-Y. Xiong, S.-B. Lu, G.-H. Yu, Q.-F. Cheng, M. Liu, Y.-R. Liang, P. Xu, X.-D. He, M. Ke, Z. Tan, and J. Luo, ZAIGA: Zhaoshan long-baseline atom interferometer gravitation antenna, *International Journal of Modern Physics D*, 1940005 (2019).
- [41] M. Abe, P. Adamson, M. Borcean, D. Bortoletto, K. Bridges, S. P. Carman, S. Chattopadhyay, J. Coleman, N. M. Curfman, K. DeRose, T. Deshpande, S. Dimopoulos, C. J. Foot, J. C. Frisch, B. E. Garber, S. Geer, V. Gibson, J. Glick, P. W. Graham, S. R. Hahn, R. Harnik, L. Hawkins, S. Hindley, J. M. Hogan, Y. Jiang, M. A. Kasevich, R. J. Kellett, M. Kiburg, T. Kovachy, J. D. Lykken, J. March-Russell, J. Mitchell, M. Murphy, M. Nantel, L. E. Nobrega, R. K. Plunkett, S. Rajendran, J. Rudolph, N. Sachdeva, M. Safdari, J. K. Santucci, A. G. Schwartzman, I. Shipsey, H. Swan, L. R. Valerio, A. Vasonis, Y. Wang, and T. Wilkason, Matter-wave Atomic Gradiometer Interferometric Sensor (MAGIS-100), *Quantum Science and Technology* **6**, 044003 (2021).
- [42] I. Dutta, D. Savoie, B. Fang, B. Venon, C. G. Alzar, R. Geiger, and A. Landragin, Continuous cold-atom inertial sensor with 1 nrad/sec rotation stability, *Phys. Rev. Lett.* **116**, 183003 (2016).